Crystal Structure of *Arabidopsis* PII Reveals Novel Structural Elements Unique to Plants[†,‡]

Yutaka Mizuno, Byron Berenger, Greg B. G. Moorhead, and Kenneth K.-S. Ng*

Department of Biological Sciences, University of Calgary, Calgary, Alberta, Canada T2N 1N4

Received October 16, 2006; Revised Manuscript Received December 7, 2006

ABSTRACT: The 1.9 Å resolution crystal structure of PII from *Arabidopsis thaliana* reveals for the first time the molecular structure of a widely conserved regulator of carbon and nitrogen metabolism from a eukaryote. The structure provides a framework for understanding the arrangement of highly conserved residues shared with PII proteins from bacteria, archaea, and red algae as well as residues conserved only in plant PII. Most strikingly, a highly conserved segment at the N-terminus that is found only in plant PII forms numerous interactions with the α2 helix and projects from the surface of the homotrimer opposite to that occupied by the T-loop. In addition, solvent-exposed residues near the T-loop are highly conserved in plants but differ in prokaryotes. Several residues at the C-terminus that are also highly conserved only in plants contribute part of the ATP-binding site and likely participate in an ATP-induced conformational change. Structures of PII also reveal how citrate and malonate bind near the triphosphate binding site occupied by ATP in bacterial and archaeal PII proteins.

Plants and most microorganisms have the ability to take up inorganic nitrogen from their environment and convert it to an organic form that can be used to synthesize the amino acids glutamate and glutamine. In plants, these amino acids are synthesized primarily in the chloroplast and function as the nitrogen donors to ultimately produce most other nitrogen-containing compounds in the cell (*1*). A tight regulation of nitrogen, carbon, and energy metabolism is necessary to coordinate the interface of these linked metabolic pathways. This is particularly important in the natural environment where organisms experience constantly changing growth conditions and nutrient availability.

The tight control of nitrogen metabolism was first revealed through studies on *E. coli* glutamine synthetase and its feedback inhibition by downstream products. A protein named PII was found to control the activity of the enzyme adenylyltransferase, which covalently modifies and regulates glutamine synthetase. This original observation in *E. coli* opened the door to the elucidation of the PII signaling cascade that coordinates the cellular response to ATP, carbon, and nitrogen status (*2*). *E. coli* PII allosterically senses ATP and 2-oxoglutarate and integrates the cellular nitrogen status signal by covalent modification (uridylylation). It then signals this information to downstream proteins, leading to alterations in the activity of glutamine synthetase and transcription of a nitrogen sensitive regulon. The PII of cyanobacteria differs in its means of covalent modification (phosphorylation, not uridylylation) and has a novel set of interacting proteins (*3*).

The PII gene, *glnb*, has been noted in essentially every archaeal and bacterial genome sequenced (*1*, *4*). A PII-like protein was discovered in the genome of the model higher plant *Arabidopsis thaliana* (*5*), and characterization has revealed that this PII protein also allosterically senses carbon status through 2-oxoglutarate and energy via ATP (*6*, *7*). No covalent modification has been detected under any nutritional condition tested (*8*). Plant PII is localized to the chloroplast (*5*, *9*), and PII knockout plants show increased sensitivity to nitrite (*10*). We and an independent research group recently discovered the first plant PII interacting protein, *N*-acetylglutamate kinase (NAGK[1]) and characterized its properties when associated with PII (*11*, *12*), confirming an interaction seen earlier during yeast two-hybrid studies (*9*, *13*). NAGK catalyzes the rate-limiting step in the pathway of arginine synthesis and when bound to PII displays an activated V_{max} and relief of inhibition by the final pathway product, arginine.

Although PII structures have been determined from several prokaryotes (*14*−*22*), there is at present no 3D structural information on PII from eukaryotes. In the prokaryotic PII structures, three copies of a protomer containing a highly conserved double $\beta-\alpha-\beta$ fold are arranged to form a cylinder. A long loop of ∼20 residues (T-loop) connects the β2 and β3 strands of each protomer and projects from a common face of the cylindrical trimer. The covalent modification of highly conserved Tyr and Ser residues near the center of this loop by uridylylation and phosphorylation in different species of *Proteobacteria* and *Cyanobacteria* affects interactions between PII and target enzymes (*4*).

We have solved the first structure of a eukaryotic PII protein, allowing us to compare the structures of a critical

[†] This work was supported by grants from the Natural Sciences and Engineering Research Council of Canada, the Alberta Ingenuity Centre for Carbohydrate Science, Canadian Institutes for Health Research, Alberta Heritage Foundation for Medical Research, and Canadian Foundation for Innovation.

[‡] Protein Data Bank codes for the reported structures are 2O66 and 2O67 for the citrate and malonate complexes, respectively.

* To whom correspondence should be addressed. Tel: 403-220-4320. Fax: 403-289-9311. E-mail: ngk@ucalgary.ca.

[1] Abbreviations: NAGK, *N*-acetylglutamate kinase.

10.1021/bi062149e CCC: $37.00
Published on Web 01/18/2007

regulatory protein at the interface of carbon and nitrogen metabolism across the domains of life. Most strikingly, peptide segments at the N- and C-termini of each protomer are unique to and highly conserved in plant PII proteins. The plant-specific N-terminal segment forms a well-defined structure on the surface of the PII trimer that may be involved with protein−protein interactions, and the plant-specific C-terminal tail likely mediates part of the protein's conformational change in response to the binding of ATP.

EXPERIMENTAL PROCEDURES

Protein Expression and Purification. A pET-3a expression plasmid was used to express a recombinant form of *A. thaliana* PII lacking the transit peptide and containing a non-natural N-terminal methionine residue preceding the full mature sequence (*8*, *11*). Apart from the addition of the N-terminal methionine, the sequence of recombinant PII produced from *E. coli* is identical to that of mature, processed *A. thaliana* PII as characterized by mass spectrometry and Edman degradation N-terminal sequencing (*8*). *E. coli* Rosetta-gami (DE3) pLysS (Novagen) was used as an expression host. Transformed cells were grown in 1.5 L terrific broth (Difco), induced with 0.5 mM IPTG, and grown for an additional 15 h at 25 °C. Cells were harvested by centrifugation, resuspended in 40 mL of 25 mM NaHEPES (pH 7.0), 50 mM NaCl, and 1 mM EDTA, and frozen at −70 °C. Cells were lysed by sonication in the presence of DNase I, and the extract was clarified by centrifugation at 27,000*g* for 30 min at 4 °C in a Sorvall SS-34 rotor. PII was further purified by cation exchange (2.5 × 4 cm column, Macro-Prep High S, Bio-Rad, elution with 0−1 M NaCl, yield ∼10 mg) and hydrophobic interaction chromatography (2.5 × 4 cm column, Phenyl-Sepharose, Amersham Biosciences, elution with 1−0 M ammonium sulfate, yield ∼6 mg) (Supporting Information, Figure S1). The protein was dialyzed against 25 mM NaHEPES (pH 7.0), 30 mM NaCl, and 5% (w/v) glycerol and concentrated to 10 mg/mL using centrifugal concentrators (Millipore Ultrafree, 5000 molecular weight cutoff).

Crystallization and Structure Determination. PII was crystallized using the hanging-drop vapor diffusion method at room temperature by mixing 1 μL of PII with an equal volume of reservoir solution containing 1.4 M tri-ammonium citrate at pH 7.0 and 10% glycerol. Small crystals of PII were used as macro-seeds and allowed to grow for about 10 days. Some crystals were also soaked into a solution containing 2.5 M malonate, 0.1 M NaHEPES at pH 7.0, and 10% glycerol.

Prior to X-ray diffraction analysis, a crystal (0.2 × 0.2 × 0.1 mm^3) was scooped up with a nylon loop and flash-cooled in a nitrogen gas stream at 100 K. Diffraction data were measured using a Rigaku RU-H3R X-ray generator and a Mar345 image plate detector. Data were processed and scaled using DENZO, SCALEPACK (*23*), and programs from CCP4 (version 5.0.2) (*24*). Autoindexing and data reduction indicated that the crystal belongs to space group *C*2. Crystallographic statistics are summarized in Table 1.

The structure of PII was determined by molecular replacement using the structure of PII from the cyanobacterium *Synechocystis* sp. PCC 6803 (pdb file: 1UL3) (*19*) as the search model (∼50% sequence identity). The solvent content of the crystals was calculated to be 35% (V_m = 1.9 Å^3/Da) if a single PII trimer were present in the asymmetric unit. Molecular replacement calculations were carried out using PHASER (*25*). The cross-rotation function gave three prominent solutions, each of which gave a single prominent translation function solution. The *R*-factor (R = 0.44, resolution = 20−3.2 Å) following rigid-body refinement was reasonable. This initial structure was refined using REFMAC (v. 5.1.24, atomic positions and temperature factors) (*26*) and manually modified using Xfit and MIFit (*27*). 89.8% of residues lie in the most favored regions of the Ramachandran plot, and no residues are in disallowed regions (PROCHECK (*28*)). A crystal of PII soaked in malonate as described above was also subjected to diffraction analysis. The crystal was isomorphous to the crystal grown from citrate, and the structure was refined starting from the refined structure of the crystal grown from citrate. The Figures were prepared with PyMOL (*29*).

Table 1: X-ray Diffraction and Refinement Statistics

	citrate complex	malonate complex
unit cell lengths (Å)	92.71, 66.75, 61.74	92.59, 66.73, 61.49
unit cell angles (°)	90, 118.9, 90	90, 118.4, 90
resolution (Å)	20−1.9	20−2.5
total reflections[a]	86074 (6815)	52167 (4596)
unique reflections[a]	25717 (2469)	11464 (1139)
redundancy[a]	3.3 (2.8)	4.6 (4.0)
completeness (%)[a]	99.2 (95.3)	99.7 (98.2)
I/σ[a]	24.0 (5.0)	14.2 (2.4)
R_{sym}[a,b]	0.051 (0.244)	0.104 (0.517)
R_{work}[c]	0.191 (0.224)	0.201 (0.249)
R_{free}[d]	0.225 (0.284)	0.266 (0.408)
number of atoms		
protein	2509	2477
ligand	39	21
solvent and ions	153	30
r.m.s. deviations from ideal geometry		
bond lengths (Å)	0.007	0.008
bond angles (°)	1.03	1.04
avg. temp. factors (Å^2)		
Wilson plot	18.5	41.9
protein	24.6	42.9
ligand	37.0	58.5
water	32.9	46.6

[a] The values from the outermost resolution shell (citrate: 1.97−1.90; malonate: 2.59−2.50) are given in parentheses. [b] $R_{sym} = \sum_h \sum_i(|I_i(h) - \langle I(h)\rangle|)/\sum_h \sum_i I_i(h)$, where $I_i(h)$ is the i^{th} integrated intensity of a given reflection, and $\langle I(h)\rangle$ is the weighted mean of all measurements of $I(h)$. [c] $R_{work} = \sum_h||F(h)_o| - |F(h)_c||/\sum_h|F(h)_o|$ for 95% of the reflection data used in refinement. [d] $R_{free} = \sum_h||F(h)_o| - |F(h)_c||/\sum_h|F(h)_o|$ for 5% of the reflection data excluded from refinement.

RESULTS

Overall Structure of Arabidopsis thaliana PII. Plant PII was expressed and crystallized minus its transit peptide as the mature form that exists in chloroplasts (*6*, *8*). A non-tagged form of the protein was purified by cation exchange chromatography and hydrophobic interaction chromatography with yields of approximately 10 mg of purified protein/L cell culture (Supporting information, Figure S1). The crystal structure of *A. thaliana* PII was determined to 1.9 Å resolution with the molecular replacement technique (Table 1). A homotrimer of 15 kDa subunits is found in the asymmetric unit of the crystal, and each subunit is composed of a double $\beta-\alpha-\beta$ motif in which a four-stranded anti-

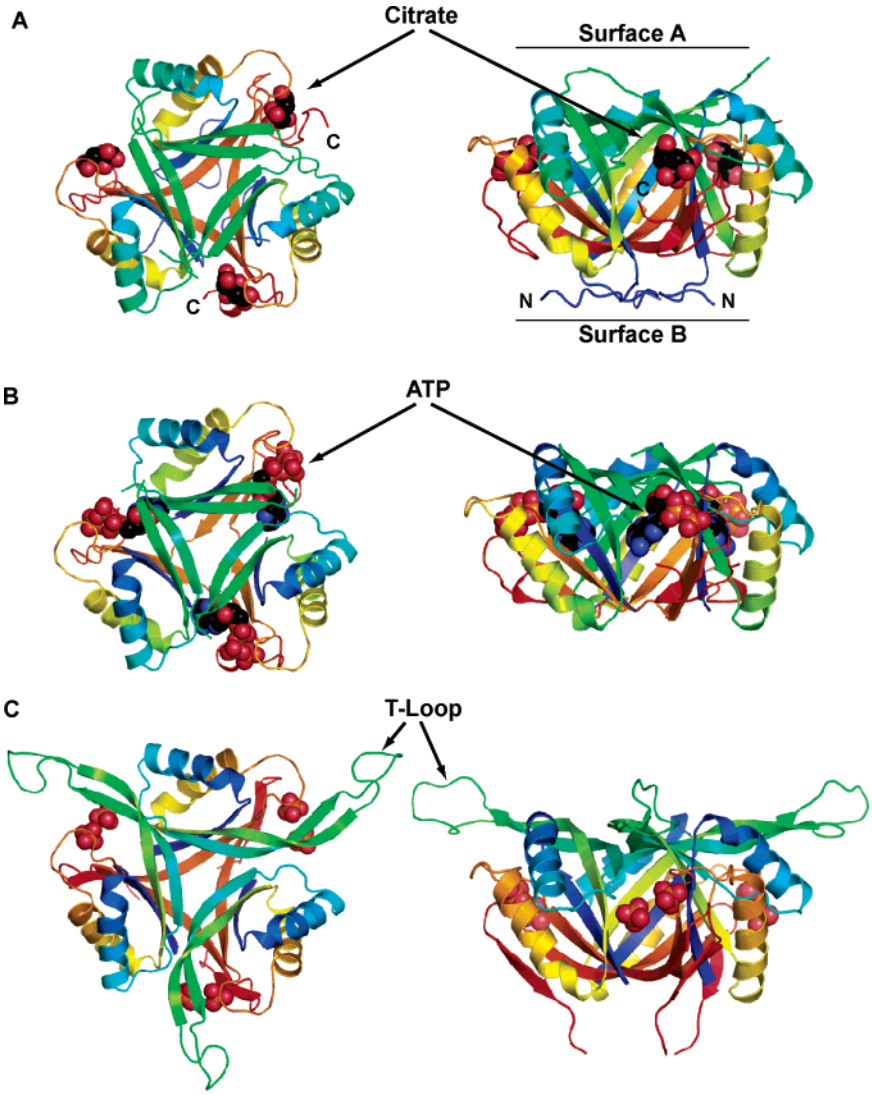

FIGURE 1: Ribbon diagrams of (A) *Arabidopsis thaliana* PII bound to citrate, (B) *E. coli* GlnK bound to ATP (2GNK (*16*)), and (C) *Synechococcus* sp. PCC 7942 PII bound to sulfate (1QY7 (*19*)). Each protomer is drawn in ribbon representation with rainbow coloring in which the N-terminus is blue, and the C-terminus is red. Citrate, ATP, and sulfate are drawn in space-filling representation. On the left, the trimer is viewed from the top, down the three-fold rotation axis of the trimer. On the right, the trimer is viewed from the side, perpendicular to the three-fold axis.

parallel β-sheet is packed against two α-helices (Figure 1A). In the biologically relevant trimer, which is also seen in solution (*6*), each edge of the β-sheet in each subunit is paired with an edge of a β-sheet from an adjacent subunit, resulting in the formation of a central trefoil core comprising 12 antiparallel β-strands. This central barrel provides a platform for presenting two distinct surfaces (designated *A* and *B* as described below) that are normal to the three-fold axis and likely mediate protein−protein interactions.

The long T-loop connecting the β2 and β3 strands in each protomer projects from surface *A*. In the *A. thaliana* PII crystal structure, this loop appears to be mostly disordered (residues 49−63, 49−64, and 48−64 in subunits A, B, and C, respectively). Disordered T-loops have also been found in the crystal structures of PII from various archaea and eubacteria (*14*−*22*). A few crystal forms of *E. coli*, *Synechococcus*, and *Thermotoga* PII contain crystal-packing interactions that appear to stabilize specific conformations of the T-loop, but it is unlikely that well-defined conformations are adopted by this loop in unbound forms of PII in solution. Post-translational modifications and mutational analysis indicate that this loop plays an important role in mediating interactions between PII and downstream-effector proteins in prokaryotes (*3*, *4*) and probably also in eukaryotes.

It is interesting to note that although most of the residues that are highly conserved in all eukaryotic and prokaryotic PII proteins involve buried residues forming the hydrophobic core and intersubunit contacts of the trimer (*14*, *16*), a number of residues are highly conserved only in plants (Figure 2). For example, Trp 22, Arg 37, and Asp 65 (using the numbering of the mature form of PII) are highly conserved in plants but differ in bacteria, archaea, and red algae. These residues are intriguingly located on the surface of the PII trimer near the T-loop and may participate in the plant-specific intermolecular interactions involved in the regulation of carbon and nitrogen metabolism. In addition, as described below, residues in plant-specific N- and C-terminal segments as well as residues at internal positions that interact with these segments are found only in plants and show a high degree of conservation only within plant PII proteins. Notably, PII from the eukaryote *Porphyra purpurea* (red algae) lacks these plant-specific features and

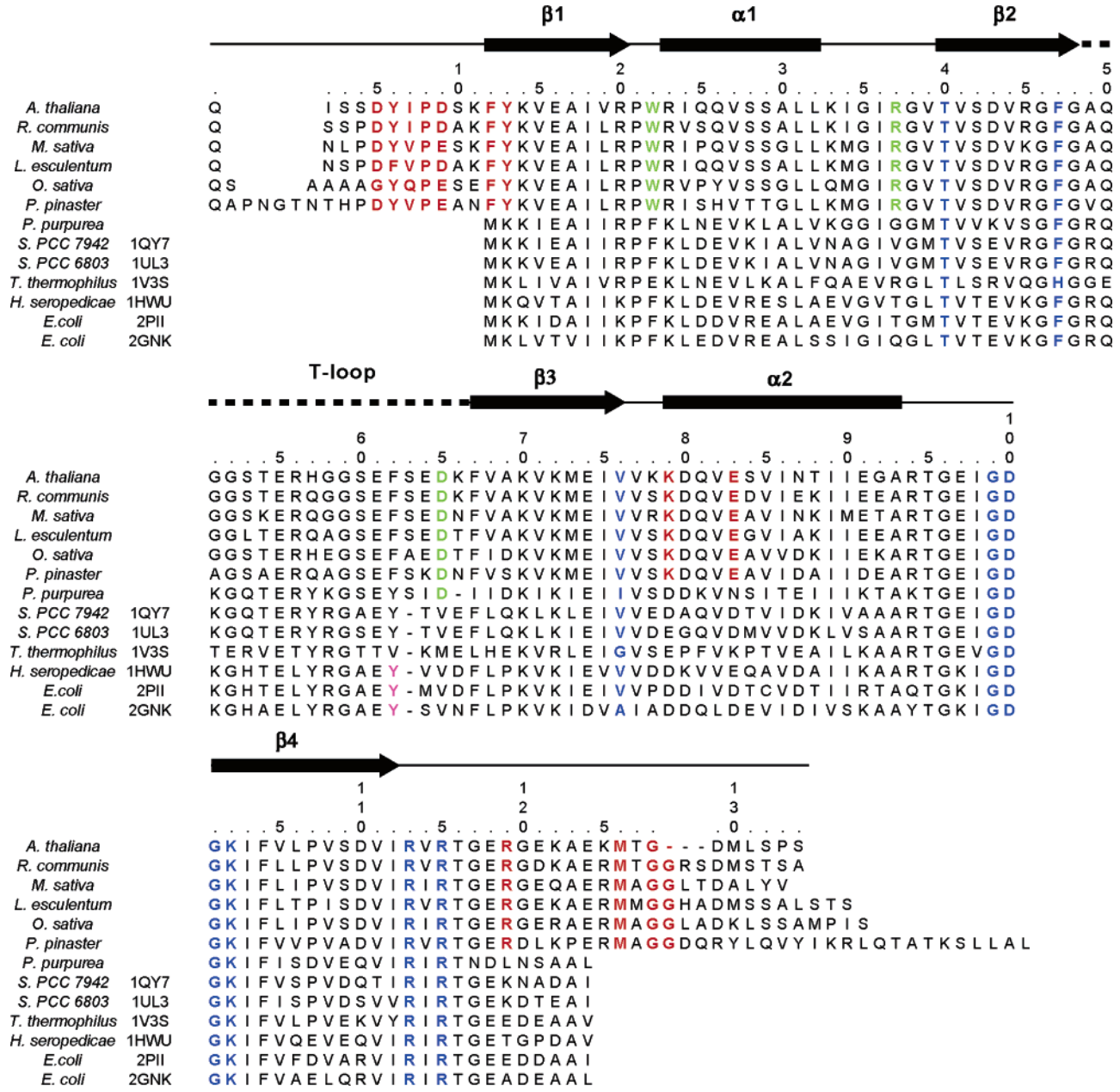

FIGURE 2: Sequence alignments of PII from plants (*Arabidopsis thaliana*, *Ricinus communis*, *Medicago sativa*, *Lycopersicon esculentum*, *Oryza sativa*, and *Pinus pinaster*), red algae (*Porphyra purpurea*), cyanobacteria (*Synechococcus* sp. PCC 7942 and *Synechocystis* sp. PCC 6803), archaebacteria (*Thermus thermophilus*), and bacteria (*Herbaspirillum seropedicae*, *Eschericia coli* GlnB (2PII) and GlnK (1GNK)). PDB identifiers have been added to identify some of the 3D structures that are currently available. Highly conserved plant-specific residues at the N- and C-termini as well as internal residues that directly interact are colored red. Highly conserved plant-specific residues that differ from those found in archaea, bacteria, and red algae are colored green. Highly conserved residues involved with the binding of ATP are colored blue. The tyrosine residue that is uridylylated in the T-loops of *E. coli* and *H. seropedicae* PII are colored in magenta.

is more similar to the PII proteins from bacteria and archaea. Intriguingly, PII from red algae is encoded in the chloroplast, whereas PII from higher plants is encoded in the nuclear genome.

Structure of the Highly Conserved Plant-Specific N-Terminal Region. The N-terminal 13 amino acids of *A. thaliana* PII form a structure that projects from surface *B* of the trimer (Figure 3). This segment is highly conserved in plants but is absent in archaea, bacteria, and red algae. Residues 5−13 form numerous interactions with residues near the C-terminal end of the α2 helix and the C-terminus of the same protomer. Lys 79, which is perfectly conserved in all plant PII proteins but is poorly conserved in all archaeal and bacterial PII proteins, lies near the end of α2 and forms numerous interactions with highly conserved residues at the N-terminus. The hydrophobic aliphatic portion of Lys 79 packs against the large aromatic side chains of Tyr 6 and Tyr 13, whereas the positively charged amino group donates hydrogen bonds to the negatively charged side chains of Asp 5 and Asp 9. Lys 11 also forms a salt bridge with Glu 121 at the C-terminus, and both of these residues are highly conserved only in plant PII. Finally, Pro 8, which is perfectly conserved in plant PII but absent in bacterial and archaeal PII, is preceded by a *cis*-peptide bond that causes the polypeptide backbone to adopt a sharp turn near the trimer three-fold axis. This sharp turn is required to position the N-terminal residues appropriately for forming all of the interactions described above, further supporting the idea that

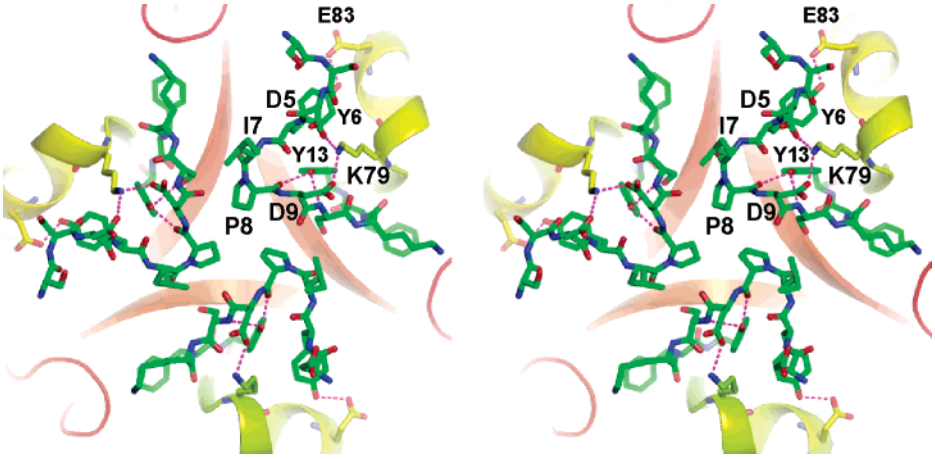

FIGURE 3: Stereoscopic view of the N-terminal region of *A. thaliana* PII. Hydrogen bonds are drawn as dashed magenta lines. Nitrogen atoms are colored blue, and oxygen atoms are colored red.

the 3D structure of this N-terminal segment is highly conserved in eukaryotic PII proteins and may play a significant biological role.

Structure of the Plant-Specific C-Terminal Region. Sequence analysis indicates that plant PII proteins contain a C-terminal segment not found in PII proteins from archaea and bacteria. The C-terminus of *A. thaliana* PII is located near the ATP-binding site and displays slightly different structures in different protomers (Figures 1 and 4). The structure is well-ordered up to residue Glu 124 in all three protomers, but the remaining 10 residues appear to be disordered in two of the protomers. In the third protomer, the C-terminal segment is well-ordered up to Met 130. Met 126, which is conserved in all plant PII proteins, anchors the C-terminal segment by occupying the hydrophobic portion of the ATP-binding site normally occupied by the adenine residue (Figure 4). This suggests that in the absence of ATP, the C-terminal segment of plant PII proteins may at least transiently occupy the ATP-binding site and that this segment may adopt a different conformation when ATP is bound. Because this C-terminal segment is only found in plant PII proteins, these structural observations suggest that ATP-dependent conformational changes in the C-terminal segment may be involved with ATP-dependent signaling mechanisms that are again unique to plants.

It should be noted that the more highly ordered C-terminal segment in this protomer appears to be stabilized by packing interactions with an adjacent molecule in the crystal lattice. The higher levels of disorder seen in the C-terminal segments of the other two protomers of *A. thaliana* PII suggest that the C-terminal segment may display a range of conformations when PII is free in solution, but this segment may possibly be stabilized by interactions with PII-effector proteins.

Interactions with Citrate and Malonate. A. thaliana PII could only be crystallized in the presence of high concentrations of either citrate or malonate, even though extensive crystallization screens and post-crystallization soaking trials were performed using low-salt conditions in the presence of polymeric precipitants in both the presence and absence of natural effectors ATP and 2-oxoglutarate. Citrate and malonate bind in a positively charged pocket that has previously been shown to bind to the triphosphate moiety of ATP (*16*, *17*, *21*) and sulfate anions (*19*) in PII proteins from bacteria and archaea (Figure 4). Although the physiological relevance

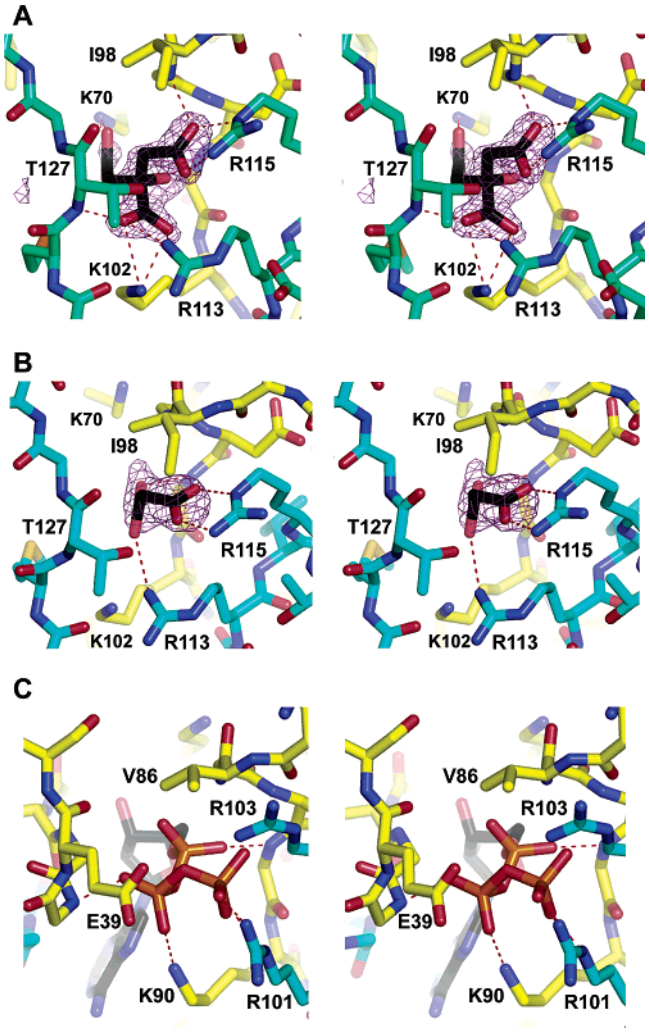

FIGURE 4: Stereoscopic view of the binding interactions for (A) citrate and (B) malonate in *A. thaliana* PII. (C) View of ATP binding to *Thermus thermophilus* PII (1V3S (*21*)) from an orientation similar to that used for panels A and B. Hydrogen bonds are drawn as dashed red lines. Separate protomers are colored yellow and cyan. Simulated-annealing omit electron density maps contoured at 3σ are drawn around the citrate and malonate ligands.

of the binding of citrate and malonate to PII is not known, the similarity of the binding of these polyvalent anions to the triphosphate moiety of ATP suggests that these anions may be competitive inhibitors of ATP binding. Indeed,

attempts to introduce ATP into *A. thaliana* PII crystals by cocrystallization or soaking at concentrations of up to 50 mM were unsuccessful.

The binding of ATP or polyanions to bacterial and archaeal PII proteins does not induce a large conformational change in the structure of the protein, but does alter the interactions of PII with effector proteins (*3*, *4*). The structural basis underlying ATP-dependent signaling is not yet known, but it is likely that the binding of ATP near the C-terminus and T-loop stabilizes a conformation in these parts of the protein that favors interactions with effector proteins mediated by surface *A*. The ATP-binding site is more distant from the N-terminal region discussed above, and ATP-binding would be expected to affect potential interactions mediated by surface *B* only through indirect means, as discussed below.

DISCUSSION

The structure of PII from *A. thaliana* reveals a number of features that are highly conserved in the sequences of a wide range of plant PII proteins but that are absent from the sequences and structures of PII proteins from bacteria, archaea, and red algae. Most striking among these plant-specific features are several highly conserved solvent-exposed residues lying near the T-loops and unique N- and C-terminal structures. The solvent-exposed residues and the C-terminal segment are located on surface *A* of the PII trimer, which suggests that these structures may be involved with ATP- or 2-oxoglutarate-dependent intermolecular interactions near the T-loop.

Because the N-terminal segment is located on the opposite side of the trimer, surface *B*, intermolecular interactions involving this segment may be less sensitive to the binding of ATP or 2-oxoglutarate. This suggests that the N-terminal segment may mediate intermolecular interactions that are either sensitive to different metabolites or perhaps insensitive to small-molecule metabolites. It should also be noted, however, that the N-terminal segment forms numerous interactions with the α2 helix of the same protomer and the C-terminal β4 strand of the adjacent protomer, which in turn interact with the ATP-binding site and T-loop. As a result, conformational changes involving ATP-binding or T-loop interactions may be transmitted indirectly to the N-terminal segment via intermediate secondary structural elements.

Although the functions of the plant-specific portions of PII are not understood at present, the structure of *A. thaliana* PII suggests approaches to elucidating these functions. For example, the solvent-exposed Trp 22, Arg 37, and Asp 65 residues that are highly conserved among plant PII proteins could be replaced with Ala or other amino acids lacking the hydrophobicity or charge of the native side chains without affecting the overall structure of PII. Such mutations would be expected to interfere with a specific aspect of PII signaling that may be unique to plants. Similarly, it may be informative to mutate Ile 7, which is a highly conserved hydrophobic residue projecting from the N-terminal region and surface *B*. Replacing this hydrophobic residue with Ser, Thr, or Asp would be expected to dramatically alter the properties of surface *B* without altering the stability, fold, or quarternary structure of the protein.

The structural basis of interactions between PII proteins and effector enzymes like NAGK remains poorly understood (*11*, *12*). The molecular structure of *A. thaliana* PII provides a starting point for understanding such intermolecular interactions. The homohexameric structures of NAGK from *Pseudomonas aeruginosa* and *Thermotoga maritima* both contain D3 symmetry, in which homodimers are arranged about a three-fold rotational axis (*30*). The conservation of residues involved in intersubunit contacts among the bacterial, archaeal, and plant PII proteins as well as the observation of a hexameric form of plant NAGK by gel filtration chromatography also suggests that plant NAGK may adopt a similar oligomeric structure (*11*). The molecular dimensions and symmetry of the PII trimer suggest that the three-fold rotational axes of NAGK and PII may align during complex formation. A more definitive understanding of this process will have to await the results of future mutagenesis and structural studies.

ACKNOWLEDGMENT

We are grateful to Dr. Isabelle Barrette-Ng for helpful discussions regarding this manuscript.

SUPPORTING INFORMATION AVAILABLE

SDS−polyacrylamide gel electrophoretograms used to evaluate the purity of PII samples used for crystallization. This material is available free of charge via the Internet at http://pubs.acs.org.

REFERENCES

1. Moorhead, G. B., and Smith, C. S. (2003) Interpreting the plastid carbon, nitrogen, and energy status. A role for PII? *Plant Physiol. 133*, 492−498.
2. Stadtman, E. R. (2001) The story of glutamine synthetase regulation, *J. Biol. Chem. 276*, 44357−44364.
3. Forchhammer, K. (2004) Global carbon/nitrogen control by PII signal transduction in cyanobacteria: from signals to targets, *FEMS Microbiol. Rev. 28*, 319−333.
4. Arcondeguy, T., Jack, R., and Merrick, M. (2001) P(II) signal transduction proteins, pivotal players in microbial nitrogen control, *Microbiol. Mol. Biol. Rev. 65*, 80−105.
5. Hsieh, M. H., Lam, H. M., van de Loo, F. J., and Coruzzi, G. (1998) A PII-like protein in *Arabidopsis*: putative role in nitrogen sensing, *Proc. Natl. Acad. Sci. U.S.A. 95*, 13965−13970.
6. Smith, C. S., Zaplachinski, S. T., Muench, D. G., and Moorhead, G. B. (2002) Expression and purification of the chloroplast putative nitrogen sensor, PII, of *Arabidopsis thaliana*, *Protein Expression Purif. 25*, 342−347.
7. Smith, C. S., Weljie, A. M., and Moorhead, G. B. (2003) Molecular properties of the putative nitrogen sensor PII from *Arabidopsis thaliana*, *Plant J. 33*, 353−360.
8. Smith, C. S., Morrice, N. A., and Moorhead, G. B. (2004) Lack of evidence for phosphorylation of *Arabidopsis thaliana* PII: implications for plastid carbon and nitrogen signaling, *Biochim. Biophys. Acta 1699*, 145−154.
9. Sugiyama, K., Hayakawa, T., Kudo, T., Ito, T., and Yamaya, T. (2004) Interaction of N-acetylglutamate kinase with a PII-like protein in rice, *Plant Cell Physiol. 45*, 1768−1778.
10. Ferrario-Mery, S., Bouvet, M., Leleu, O., Savino, G., Hodges, M., and Meyer, C. (2005) Physiological characterisation of *Arabidopsis* mutants affected in the expression of the putative regulatory protein PII, *Planta 223*, 28−39.
11. Chen, Y. M., Ferrar, T. S., Lohmeir-Vogel, E., Morrice, N., Mizuno, Y., Berenger, B., Ng, K. K., Muench, D. G., and Moorhead, G. B. (2006) The PII signal transduction protein of *Arabidopsis thaliana* forms an arginine-regulated complex with plastid N-acetyl glutamate kinase, *J. Biol. Chem. 281*, 5726−5733.
12. Ferrario-Mery, S., Besin, E., Pichon, O., Meyer, C., and Hodges, M. (2006) The regulatory PII protein controls arginine biosynthesis in *Arabidopsis*, *FEBS Lett. 580*, 2015−2020.
13. Burillo, S., Luque, I., Fuentes, I., and Contreras, A. (2004) Interactions between the nitrogen signal transduction protein PII

and N-acetyl glutamate kinase in organisms that perform oxygenic photosynthesis, *J. Bacteriol. 186*, 3346−3354.

14. Cheah, E., Carr, P. D., Suffolk, P. M., Vasudevan, S. G., Dixon, N. E., and Ollis, D. L. (1994) Structure of the *Escherichia coli* signal transducing protein PII, *Structure 2*, 981−990.
15. Carr, P. D., Cheah, E., Suffolk, P. M., Vasudevan, S. G., Dixon, N. E., and Ollis, D. L. (1996) X-ray structure of the signal transduction protein from *Escherichia coli* at 1.9 Å, *Acta Crystallogr., Sect. D 52*, 93−104.
16. Xu, Y., Cheah, E., Carr, P. D., van Heeswijk, W. C., Westerhoff, H. V., Vasudevan, S. G., and Ollis, D. L. (1998) GlnK, a PII-homologue: structure reveals ATP binding site and indicates how the T-loops may be involved in molecular recognition, *J. Mol. Biol. 282*, 149−165.
17. Xu, Y., Carr, P. D., Huber, T., Vasudevan, S. G., and Ollis, D. L. (2001) The structure of the PII-ATP complex, *Eur. J. Biochem. 268*, 2028−2037.
18. Machado Benelli, E., Buck, M., Polikarpov, I., Maltempi de Souza, E., Cruz, L. M., and Pedrosa, F. O. (2002) *Herbaspirillum seropedicae* signal transduction protein PII is structurally similar to the enteric GlnK, *Eur. J. Biochem. 269*, 3296−3303.
19. Xu, Y., Carr, P. D., Clancy, P., Garcia-Dominguez, M., Forchhammer, K., Florencio, F., Vasudevan, S. G., Tandeau de Marsac, N., and Ollis, D. L. (2003) The structures of the PII proteins from the cyanobacteria *Synechococcus* sp. PCC 7942 and *Synechocystis* sp. PCC 6803, *Acta Crystallogr., Sect. D 59*, 2183−2190.
20. Schwarzenbacher, R., von Delft, F., Abdubek, P., Ambing, E., Biorac, T., Brinen, L. S., Canaves, J. M., Cambell, J., Chiu, H. J., Dai, X., Deacon, A. M., DiDonato, M., Elsliger, M. A., Eshagi, S., Floyd, R., Godzik, A., Grittini, C., Grzechnik, S. K., Hampton, E., Jaroszewski, L., Karlak, C., Klock, H. E., Koesema, E., Kovarik, J. S., Kreusch, A., Kuhn, P., Lesley, S. A., Levin, I., McMullan, D., McPhillips, T. M., Miller, M. D., Morse, A., Moy, K., Ouyang, J., Page, R., Quijano, K., Robb, A., Spraggon, G., Stevens, R. C., van den Bedem, H., Velasquez, J., Vincent, J., Wang, X., West, B., Wolf, G., Xu, Q., Hodgson, K. O., Wooley, J., and Wilson, I. A. (2004) Crystal structure of a putative PII-like signaling protein (TM0021) from *Thermotoga maritima* at 2.5 Å resolution, *Proteins 54*, 810−813.
21. Sakai, H., Wang, H., Takemoto-Hori, C., Kaminishi, T., Yamaguchi, H., Kamewari, Y., Terada, T., Kuramitsu, S., Shirouzu, M., and Yokoyama, S. (2005) Crystal structures of the signal transducing protein GlnK from *Thermus thermophilus* HB8, *J. Struct. Biol. 149*, 99−110.
22. Nichols, C. E., Sainsbury, S., Berrow, N. S., Alderton, D., Saunders, N. J., Stammers, D. K., and Owens, R. J. (2006) Structure of the PII signal transduction protein of *Neisseria meningitidis* at 1.85 Å resolution, *Acta Crystallogr., Sect. F 62*, 494−497.
23. Otwinowski, Z., and Minor, W. (1997) Processing of x-ray diffraction data collected in oscillation mode, *Methods Enzymol. 276*, 307−326.
24. Collaborative Computational Project, Number 4 (1994) The CCP4 suite: programs for protein crystallography, *Acta Crystallogr., Sect. D 50*, 760−763.
25. Read, R. J. (2001) Pushing the boundaries of molecular replacement with maximum likelihood, *Acta Crystallogr., Sect. D 57*, 1373−1382.
26. Murshudov, G. N., Vagin, A. A., and Dodson, E. J. (1997) Refinement of macromolecular structures by the maximum-likelihood method, *Acta Crystallogr., Sect. D 53*, 240−255.
27. McRee, D. E. (1999) XtalView/Xfit—A versatile program for manipulating atomic coordinates and electron density, *J. Struct. Biol. 125*, 156−165.
28. Morris, A. L., MacArthur, M. W., Hutchinson, E. G., and Thornton, J. M. (1992) Stereochemical quality of protein structure coordinates, *Proteins 12*, 345−364.
29. DeLano, W. L. (2002) *PyMOL*, DeLano Scientific, San Carlos, CA.
30. Ramon-Maiques, S., Fernandez-Murga, M. L., Gil-Ortiz, F., Vagin, A., Fita, I., and Rubio, V. (2006) Structural bases of feed-back control of arginine biosynthesis, revealed by the structures of two hexameric N-acetylglutamate kinases, from *Thermotoga maritima* and *Pseudomonas aeruginosa*, *J. Mol. Biol. 356*, 695−713.

BI062149E